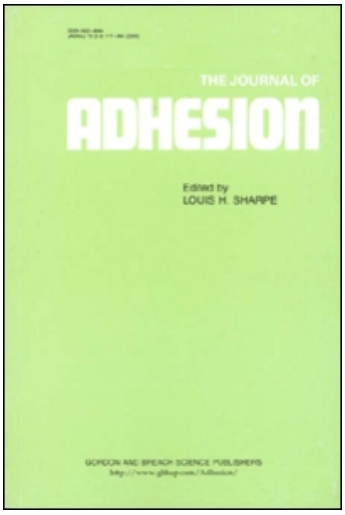

The Journal of Adhesion
Publication details, including instructions for authors and subscription information:
http://www.informaworld.com/smpp/title~content=t713453635

The Stress Intensity Factor in Bonded Quarter Planes after a Change in Temperature

M. Tilscher[a]; D. Munz[ab]; Y. Y. Yang[b]
[a] Kernforschungszentrum Karlsruhe, Karlsruhe, Germany [b] University of Karlsruhe, Karlsruhe, Germany

To cite this Article Tilscher, M. , Munz, D. and Yang, Y. Y.(1995) 'The Stress Intensity Factor in Bonded Quarter Planes after a Change in Temperature', The Journal of Adhesion, 49: 1, 1 — 21
To link to this Article: DOI: 10.1080/00218469508009974
URL: http://dx.doi.org/10.1080/00218469508009974

J. Adhesion, 1995, Vol. 49, pp. 1–21
Reprints available directly from the publisher
Photocopying permitted by license only

The Stress Intensity Factor in Bonded Quarter Planes after a Change in Temperature

M. TILSCHER,[1] D. MUNZ,[1,2] and Y. Y. YANG[2]

[1] *Kernforschungszentrum Karlsruhe, IMF II, D-76021 Karlsruhe, Germany*
[2] *University of Karlsruhe, IZSM, D-76021 Karlsruhe, Germany*

(Received March 26, 1994; in final form August 30, 1994)

High stresses can occur in bonded dissimilar materials after a change in temperature in the vicinity of the intersection of the interface and the free edge. These stresses depend on the thermal expansion and on the elastic constants of the two materials. In bonded quarter planes the stresses near the intersection of the interface and the free edge can be described by the sum of one singular term and one regular term which is independent of the distance to the singular point. With the exception of the stress intensity factor of the singular term, all parameters can be calculated analytically. The stress intensity factor was evaluated numerically using the finite element method. Joints with different ratios of height to length and various material combinations were investigated. An empirical relationship between the stress intensity factor, the elastic constants and the ratios of height to length of the joint is given by exponential and polynomial equations.

KEY WORDS: thermal stresses; bimaterial; stress singularity; stress intensity factor; FEM.

INTRODUCTION

Many engineering components contain bimaterials, *e.g.* ceramic-metal joints, in order to combine the special properties of different materials. During the fabrication process, or later in use, the bimaterial is exposed to a change in temperature. Due to the differences in thermal expansion, stresses occur in both materials. Several investigations of the thermal stresses have been published.

Timoshenko[1] conducted a stress analysis of the heated bimaterial strip using the elementary beam theory. Timoshenko's analysis predicted that a constant radius of curvature would develop along the length of the strip, and a linear axial stress distribution would be generated away from the ends of the strip. Hess[2] examined the stress distribution near the ends of the bimaterial. In his study, a stress field was assumed for the end loaded plate and superimposed on that from Timoshenko's solution to satisfy the condition of equilibrium at the free ends. Suhir[3] developed an approach based on an elementary beam associated with finite longitudinal and transverse interfacial compliances which enabled the equilibrium conditions to be satisfied at the stress-free edges. Williams[4] first described the singular stress fields with singularities of type $r^{-\omega}$. The singularity exponent, ω, as a function of the geometry at

the free edge and the elastic constants, was calculated by Bogy.[5] Heinzelmann *et al.*[6] investigated the relationship between the ratios of height to length and the stress intensity factor for joints with equal heights of both materials. In the present paper, the relationship between the stress intensity factor, the elastic constants and the ratios of height to length of bonded quarter planes will be studied.

GENERAL STRESS RELATION

For the stress analysis, the following assumptions have been made:

- Homogeneous change in temperature.
- Perfect bond at the interface.
- Plane strain.
- Both materials are linear elastic, homogeneous and isotropic. The material parameters are independent of the temperature.

Applying an Airy stress function and the appropriate boundary conditions, the components of the stress tensor in the vicinity of the intersection of the interface and the free edge of two bonded quarter planes can be described as a function of the coordinates r and θ (Fig. 1).[7]

$$\sigma_{ij}(r,\theta) = \frac{K_L}{\left(\frac{r}{L}\right)^{\omega}} f_{ij}(\theta) + \sigma_{ij0}(\theta). \tag{1}$$

For joints with two rectangular wedge angles, the stress exponent can be obtained by solving the following transcendental equation:[8]

$$\lambda^2(\lambda^2-1)\alpha^2 + 2\lambda^2[\sin^2(\pi\lambda/2) - \lambda^2]\alpha\beta + [\sin^2(\pi\lambda/2) - \lambda^2]^2\beta^2 + \sin^2(\pi\lambda/2)\cos^2(\pi\lambda/2) = 0 \tag{2}$$

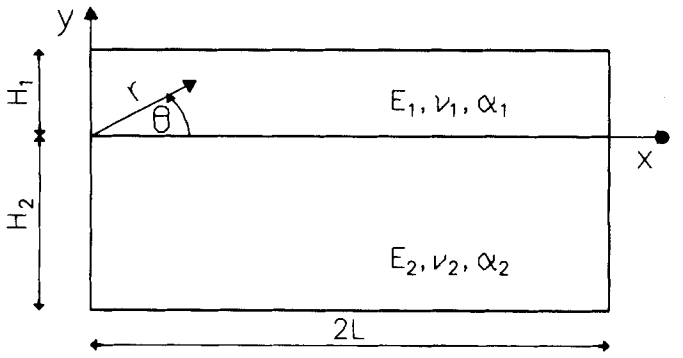

FIGURE 1 The investigated geometry of the bimaterial.

with

$$\omega = 1 - \mathrm{Re}(\lambda).$$

α and β are the Dundurs parameters,[9] which are a function of the elastic constants of the two materials L:

$$\alpha = \frac{m_2 - km_1}{m_2 + km_1} \tag{3a}$$

$$\beta = \frac{(m_2 - 2) - k(m_1 - 2)}{m_2 + km_1} \tag{3b}$$

with

$$k = \frac{G_2}{G_1}$$

and

$$m_i = \begin{cases} \dfrac{4}{(1+\nu_i)} & \text{for plane stress} \\ 4(1-\nu_i) & \text{for plane strain.} \end{cases}$$

G is the shear modulus and ν is the Poisson's ratio.

To describe the stress distribution near the singular point only stress exponents in the range $-0.5 < \omega < 1$ are of interest. Equation (2) leads to only one solution for ω in the interesting range.

The components of the regular stress tensor σ_{ij0} are:[10]

$$\sigma_{r0} = \sigma_0 \sin^2(\theta) \tag{4a}$$

$$\sigma_{\theta 0} = \sigma_0 \cos^2(\theta) \tag{4b}$$

$$\sigma_{r\theta 0} = \sigma_0 \cos(\theta)\sin(\theta) \tag{4c}$$

where σ_0 can be calculated by

$$\sigma_0 = \Delta T(\alpha_2' - \alpha_1') \frac{1}{E_2^{*-1} - E_1^{*-1}}$$

$$E_i^* = \begin{cases} \dfrac{E_i}{\nu_i} & \text{for plane stress} \\ \dfrac{E_i}{\nu_i(1+\nu_i)} & \text{for plane strain.} \end{cases}$$

$$\alpha_i' = \begin{cases} \alpha_i & \text{for plane stress} \\ \alpha_i(1+\nu_i) & \text{for plane strain.} \end{cases}$$

The equations for the angular functions f_{ij} are given by Yang.[10]

In Eq. (1) the stress intensity factor has the same dimension as the stress. For thermal loading the stress intensity factor, K_L can be written as

$$K_L = \Delta T(\alpha_2' - \alpha_1')K_1^*. \tag{5}$$

K_1^* depends on the Young's moduli, on the Poisson's ratios of the two materials, and on the geometry of the joint. K_1^* can be calculated numerically, *e.g.* by the finite element method.

For a rectangular joint with $\min(H_1/L, H_2/L) \geq 2$ the stress intensity factor, K_L, for a given material combination is constant and denoted as $K_{L\infty}$. For $-K_{L\infty}/\sigma_0$ a polynomial approximation was found[7]

$$-K_{L\infty}/\sigma_0 = 1 - 2.89\omega + 11.4\omega^2 - 51.9\omega^3 + 135.7\omega^4 - 135.8\omega^5. \tag{6}$$

Later on, deviations of up to ten percent were calculated between the values of the equation above and the results of the finite element calculation.[11] The divergence increases with decreasing stress exponent, ω, and increasing difference between the Poisson's ratios ν_1 and ν_2. For material combinations of practical relevance, with Poisson's ratios from 0.2 to 0.4, the equation above constitutes a good approximation to the stress intensity factor $K_{L\infty}$. The maximum relative error does not exceed three percent.

In this paper, the stress intensity factor is calculated for different ratios H_1/L and H_2/L and different material combinations of a joint. The relationship between the stress intensity factor, the ratios of height to length and the elastic constants are described.

FINITE ELEMENT PROCEDURE

The thermal stress field was calculated with the FE-code ABAQUS.[12] The mesh in the vicinity to the singular point is shown in Figure 2. Biquadratic elements with eight nodes and reduced integration were used. The smallest distance between two nodes referring to $\min(H_1, H_2, L)$ is 10^{-6}. All calculations are made for a decrease in temperature of one Kelvin.

The stress intensity factor was obtained from a plot of $\log(\sigma_{ij} - \sigma_{ij0})$ *versus* $\log(r/L)$. As an example, material combination A with a large ω is considered (see Table I). In Figure 3a the values of $\log(\sigma_{ij} - \sigma_{ij0})$ are plotted *versus* the relative distance $\log(r/L)$ along the interface. Figure 3b shows the values of $\log(\sigma_y - \sigma_{y0})$ along the free edge of material 1 and material 2. A straight line with the slope $-\omega$ can be seen. The stress intensity factor can be obtained from the location of any one of these lines, applying the corresponding values f_{ij} and σ_{ij0}. To determine the stress intensity factor a quantity Π is defined as

$$\Pi = \sum_{k=1}^{n} \left\{ \ln(\sigma_{ij}^{FE}(r_k, \theta_k) - \sigma_{ij0}(\theta_k)) - \ln(K_L f_{ij}(\theta_k)) + \omega \ln\left(\frac{r_k}{L}\right) \right\}^2, \tag{7}$$

where n is the number of points used to determine K_L. According to the least squares method, the minimum of Π with respect to the value K_L has to be found. It is given by

$$\frac{\partial \Pi}{\partial K_L} = 0 \tag{8}$$

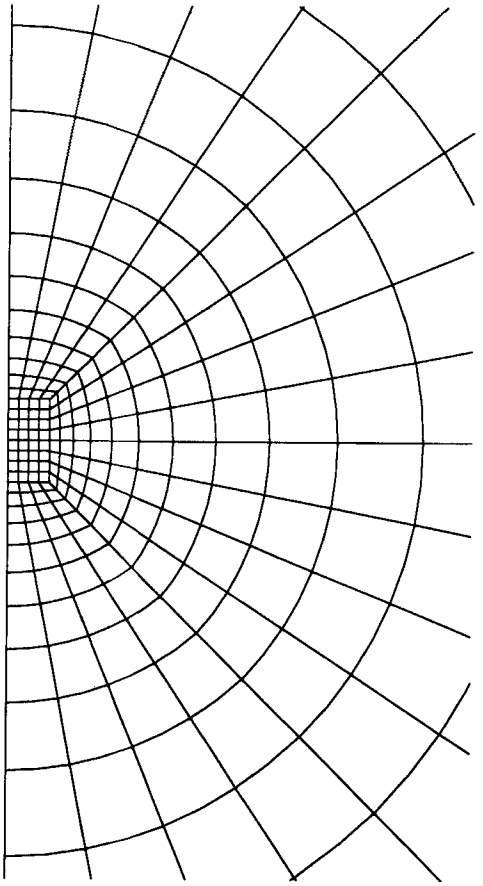

FIGURE 2 The mesh in the vicinity of the singular point.

leading to the equation

$$K_L = \frac{1}{f_{ij}(\theta_k)} \exp\left\{\frac{1}{n}\left[\sum_{k=1}^{n} \ln(\sigma_{ij}^{FE}(r_k, \theta_k) - \sigma_{ij0}(\theta_k)) + \omega \sum_{k=1}^{n} \ln\left(\frac{r_k}{L}\right)\right]\right\}, \tag{9}$$

with $\theta_k = const,$

where f_{ij}, σ_{ij0} and ω can be calculated analytically. The stresses σ_{ij}^{FE} are calculated by the finite element method.

RESULTS

Material Parameters

For a given material combination there are two possibilities to indicate the two materials with the subscript 1 and 2. We choose the indication so that it holds:

$$E_1^* > E_2^*, \tag{10}$$

TABLE Ia
Geometry and material parameters of combination A

Combination	$\frac{H_1}{H_2}$	$\frac{L}{H_2}$	E_1 in GPa	E_2 in GPa	ν_1	ν_2	α_1 in $10^{-6}K^{-1}$	α_2 in $10^{-6}K^{-1}$
A	0.5	10	250	25	0.33	0.28	1	2

TABLE Ib
The Dundurs parameters, the stress exponent, the regular stress term and the angular functions of combination A

Combination	α	β	ω	σ_0 in MPa	$f_{y0°}$	$f_{y45°}$	$f_{y90°}$
A	0.8237	0.2562	0.1864	−0.09777	1.0	1.1474	1.7990

this corresponds to

$$\beta < \alpha/2. \tag{11}$$

As another example the material parameters of combination *B* are given in Table IIa. Table IIb shows the values of the Dundurs parameters, α and β, the stress exponent, ω, and the regular stress term, σ_{ij0}. This material combination has a smaller stress exponent, ω, than combination *A*.

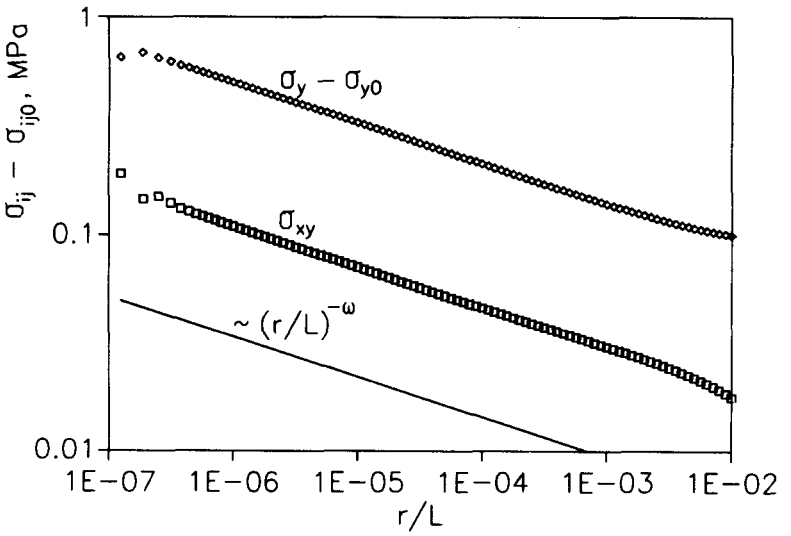

FIGURE 3a The values $\log(\sigma_y - \sigma_{y0})$ and $\log(\sigma_{xy})$ *versus* $\log(r/L)$ along the interface for combination A.

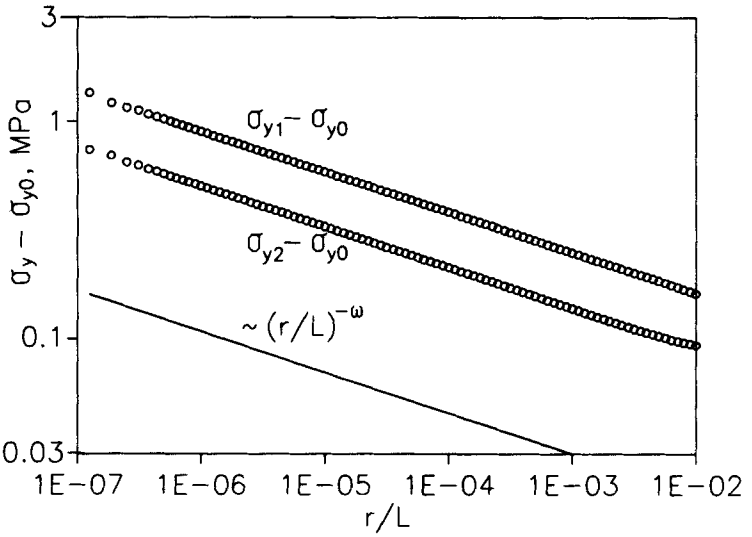

FIGURE 3b The values $\log(\sigma_y - \sigma_0)$ *versus* $\log(r/L)$ along the free edge of material 1 and material 2 for combination A.

TABLE IIa
Material parameters of combination B

Combination	E_1 in GPa	E_2 in GPa	ν_1	ν_2	α_1 in $10^{-6}K^{-1}$	α_2 in $10^{-6}K^{-1}$
B	400	70	0.3	0.2	4	8

TABLE IIb
Dundurs parameters, α and β, the stress exponent, ω, and the regular stress term, σ_{y0}, for combination B

Combination	α	β	ω	σ_{y0} in MPa
B	0.71543	0.28099	0.094733	−1.79330

Effect of Geometry

In Eq. (1), L is the half length of the joint (see Fig. 1). To normalise the distance r, the height, H_1, of material 1 or the height, H_2, of material 2 can be used as well. The corresponding stress intensity factors are then denoted K_{H1} and K_{H2}, respectively. Between the different definitions of the stress intensity factor the relationship

$$K_L L^{\omega} = K_{H1} H_1^{\omega} = K_{H2} H_2^{\omega} \tag{12}$$

holds.

The stress intensity factor for combination B was calculated using the method described above. The ratios H_1/H_2 and L/H_1 are varied. Figure 4a shows the stress

intensity factor K_{H1} *versus* L/H_1 for different ratios H_1/H_2. The same results are plotted in Figure 4b as K_{H2} *versus* L/H_2.

The relationship between the ratios of height to length of the joint and the stress intensity factor, K, can be described as follows:

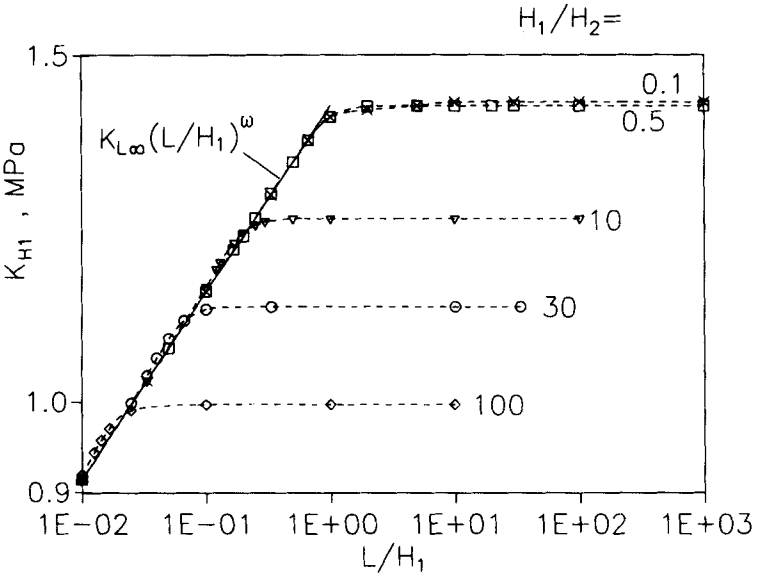

FIGURE 4a Log(K_{H1}) *versus* log(L/H_1) for combination B with different ratios H_1/H_2.

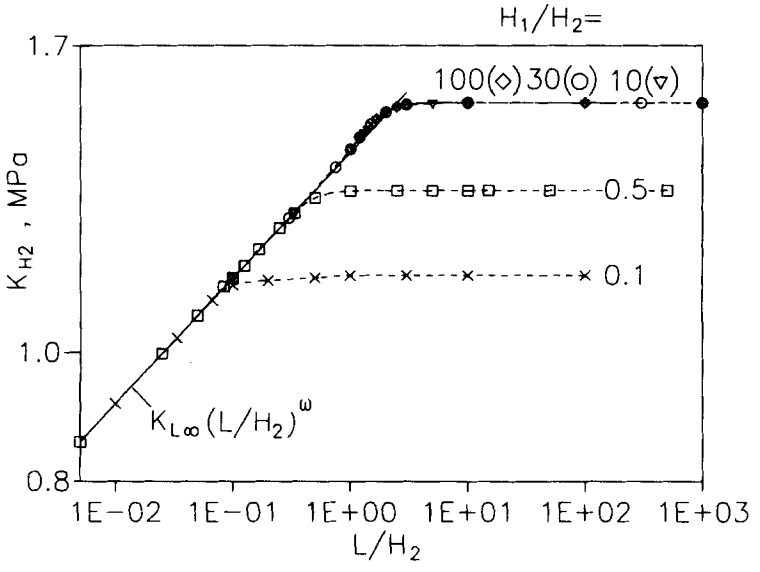

FIGURE 4b Log(K_{H2}) *versus* log(L/H_2) for combination B with different ratios H_1/H_2.

1. For joints with $\min(H_1/L, H_2/L) \geq 2$ the value of $K_L = K_{L\infty}$ is independent of H_1/L and H_2/L. Therefore,

$$K_{H1} = K_{L\infty}\left(\frac{L}{H_1}\right)^{\omega} \tag{13a}$$

$$K_{H2} = K_{L\infty}\left(\frac{L}{H_2}\right)^{\omega} \tag{13b}$$

   The value of $\log(K_{H1})$ increases linearly with $\log(L/H_1)$ (and $\log(K_{H2})$ linearly with $\log(L/H_2)$) with a slope of ω.
2. Above a critical value of L/H_1 (or L/H_2), K_{H1} (or K_{H2}) reaches a constant value, $K_{H1\infty}$ (or $K_{H2\infty}$). The critical value of L/H_1 (or L/H_2) depends on H_1/H_2.
3. The transition between the straight line with the slope ω and $K_{H1} = K_{H1\infty}$ (or $K_{H2} = K_{H2\infty}$ is continuous and takes place in a narrow range of L/H_1 (or L/H_2).

In Figure 5a $K_{H1\infty}$ is plotted *versus* H_2/H_1 and in Figure 5b $K_{H2\infty}$ is plotted *versus* H_1/H_2. It can be seen that:

1. $K_{H1\infty}$ reaches a constant value $K^*_{H1\infty}$ for $H_2/H_1 \geq 10$.
2. $K_{H2\infty}$ reaches a constant value $K^*_{H2\infty}$ for $H_1/H_2 \geq 10$.
3. $K^*_{H1\infty}$ corresponds to the location of the straight line in the $\log(K_{H2\infty}) - \log(H_1/H_2)$ plot which is given by:

$$K_{H2\infty} = K^*_{H1\infty}\left(\frac{H_1}{H_2}\right)^{\omega}. \tag{14a}$$

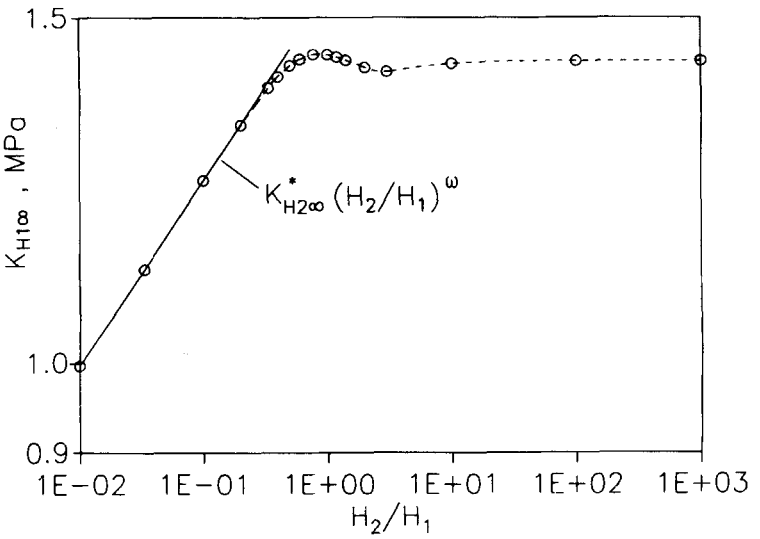

FIGURE 5a $\text{Log}(K_{H1\infty})$ *versus* $\log(H_2/H_1)$ for combination B.

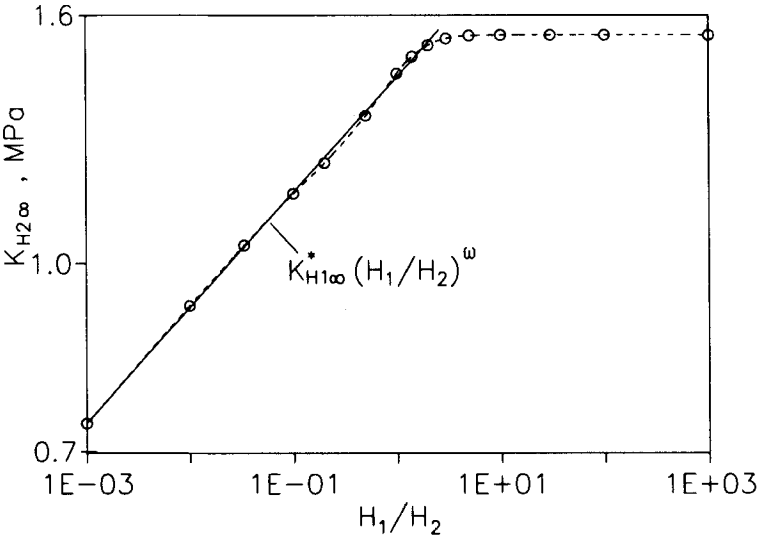

FIGURE 5b Log($K_{H2\infty}$) *versus* log(H_1/H_2) for combination B.

4. $K^*_{H2\infty}$ corresponds to the location of the straight line in the $\log(K_{H1\infty}) - \log(H_2/H_1)$ plot which is given by:

$$K_{H1\infty} = K^*_{H2\infty}\left(\frac{H_2}{H_1}\right)^{\omega}. \tag{14b}$$

5. In Figure 5, the transitions between the straight lines with the slope ω and the constant values $K^*_{H1\infty}(K^*_{H2\infty})$ are continuous and occur in a small range of $H_2/H_1(H_1/H_2)$.

The complete relationship between K_{H2} and the ratio H_2/L can be described by

$$K_{H2} = A\left[1 - \exp\left\{-\left(\frac{K_{L\infty}}{A}\right)^{n}\left(\frac{L}{H_2}\right)^{n\omega}\right\}\right]^{\frac{1}{n}} \tag{15a}$$

with

$$A = K^*_{H2\infty}\left[1 - \exp\left\{-\left(\frac{K^*_{H1\infty}}{K^*_{H2\infty}}\right)^{n}\left(\frac{H_1}{H_2}\right)^{n\omega}\right\}\right]^{\frac{1}{n}} \tag{15b}$$

where n is a curve-fitting parameter. The stresses then can be described by Eq. (1) with

$$K_L = K_{H2}\left(\frac{H_2}{L}\right)^{\omega}. \tag{16}$$

Altogether, there are three characteristic constants describing the relationship between the stress intensity factor, K, and the ratios of height to length of the joint. The

definitions of these constants are:

$$K_{L\infty} = K_L\left(\frac{H_1}{H_2}, \frac{L}{H_2}\right)\Big|_{\min(H_1/L, H_2/L) \geq 2} \tag{17a}$$

$$K^*_{H1\infty} = K_{H1}\left(\frac{H_1}{H_2}, \frac{L}{H_2}\right)\Big|_{H_1/H_2 \leq 0.1, H_1/L \leq 0.1} \tag{17b}$$

This means that the thickness of material 1 is much smaller than the thickness of material 2 and the length of the interface (thin layer of material 1 bonded to a thick substratum of material 2).

$$K^*_{H2\infty} = K_{H2}\left(\frac{H_1}{H_2}, \frac{L}{H_2}\right)\Big|_{H_2/H_1 \leq 0.1, H_2/L \leq 0.1} \tag{17c}$$

This means that the thickness of material 2 is much smaller than the thickness of material 1 and the length of the interface (thin layer of material 2 bonded to a thick substratum of material 1).

These three constants are independent of the geometry and, therefore, they are characteristic parameters for each material combination.

For some special values of the ratios $H_1/L, H_2/L$ the following relations can be used:

$$\sigma_{ij} = \frac{K_{L\infty}}{\left(\frac{r}{L}\right)^{\omega}} f_{ij}(\theta) + \sigma_{ij0}(\theta), \qquad \text{for} \quad \min(H_1/L, H_2/L) \geq 2 \tag{18a}$$

$$\sigma_{ij} = \frac{K^*_{H_1\infty}}{\left(\frac{r}{H_1}\right)^{\omega}} f_{ij}(\theta) + \sigma_{ij0}(\theta), \qquad \text{for} \quad H_1/H_2 \leq 0.1, H_1/L \leq 0.1 \tag{18b}$$

$$\sigma_{ij} = \frac{K^*_{H2\infty}}{\left(\frac{r}{H_2}\right)^{\omega}} f_{ij}(\theta) + \sigma_{ij0}(\theta), \qquad \text{for} \quad H_2/H_1 \leq 0.1, H_2/L \leq 0.1 \tag{18c}$$

Effect of the Elastic Constants

To describe the stress intensity factor K_{H2} the three constants $K_{L\infty}$, $K^*_{H1\infty}$, $K^*_{H2\infty}$ and the fitting parameter n should be determined. A polynomial approximation for $K_{L\infty}$ has already been given in Eq. (6).

THE PARAMETER $K^*_{H2\infty}$

To investigate the relationship between the elastic constants and $K^*_{H2\infty}$, the stress intensity factor is calculated by the method described before. The geometry of the joints are $H_1/H_2 = 100$ and $L/H_2 = 100$, leading to the stress intensity factor $K^*_{H2\infty}$. The

material parameters of the joints investigated are:

$$E_1 = 1 \times 10^5 \text{MPa} \qquad 0.05 \le \nu_1 \le 0.49 \qquad \alpha_1 = 1 \times 10^{-6} \text{K}^{-1}$$

$$1 \times 10^3 \text{MPa} \le E_2 \le \frac{\nu_2(1+\nu_2)}{\nu_1(1+\nu_1)} E_1 \qquad 0.05 \le \nu_2 \le 0.49 \qquad \alpha_2 = 2 \times 10^{-6} \text{K}^{-1}$$

The upper limit for E_2 is due to the restriction $\beta < \alpha/2$. The values of $-K^*_{H2\infty}/\sigma_0$ are plotted *versus* the stress exponent, ω, in Figure 6. The values K and σ_0 are proportional to ΔT and to $(\alpha'_2 - \alpha'_1)$. Therefore, the ratio $K^*_{H2\infty}/\sigma_0$ is independent of the thermal load, ΔT, and the difference of the thermal expansion coefficients. The same results as in Figure 6 are shown in Figure 7 for fixed Poisson's ratios of $\nu_2 = 0.2, 0.25$ and 0.3. It can be seen that generally $-K^*_{H2\infty}/\sigma_0$ decreases with increasing ω. For a fixed value ν_2 a more or less unique relation between $-K^*_{H2\infty}/\sigma_0$ and ω exists, even if ν_1, E_1 and E_2 are varied. All results can be fitted by a polynomial expression:

$$-K^*_{H2\infty}/\sigma_0 = 1.0137 - 0.1867\,\nu_2 - 2.8641\,\omega + 10.3654\,\nu_2\omega + 0.6783\,\nu_2^2 - 17.5983\,\nu_2^2\omega + 2.3556\,\omega^2 - 17.454\,\nu_2\omega^2 + 36.2823\,\nu_2^2\omega^2 \qquad (19)$$

The values of Eq. (19) are also shown as solid lines in Figure 7a–7c. The maximum relative error $(K^{*FE}_{H2\infty} - K^*_{H2\infty})/K^*_{H2\infty}$ between the results obtained using the FE method and Eq. (19) is smaller than 10%.

THE PARAMETER $K^*_{H1\infty}$

The geometry is $H_1/H_2 = 0.01$ and $L/H_1 = 100$ which leads to the stress intensity factor $K^*_{H1\infty}$.

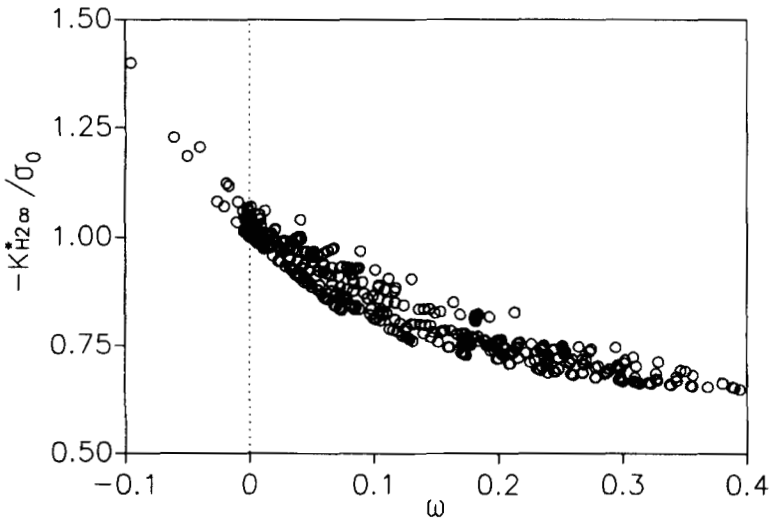

FIGURE 6 Values of $-K^*_{H2\infty}/\sigma_0$ *versus* the stress exponent, ω.

The material parameters are:

$$E_1 = 1 \times 10^5 \text{MPa} \qquad 0.05 \le \nu_1 \le 0.49 \qquad \alpha_1 = 1 \times 10^{-6}\,\text{K}^{-1}$$

$$1 \times 10^3\,\text{MPa} \le E_2 \le \frac{\nu_2(1+\nu_2)}{\nu_1(1+\nu_1)} E_1 \qquad 0.05 \le \nu_2 \le 0.49 \qquad \alpha_2 = 2 \times 10^{-6}\,\text{K}^{-1}$$

The upper limit of E_2 results from the restriction $\beta < \alpha/2$. Figure 8 shows the values of $-K^*_{H1\infty}/\sigma_0$ *versus* ω. The same results as in Figure 8 are shown in Figure 9 for fixed

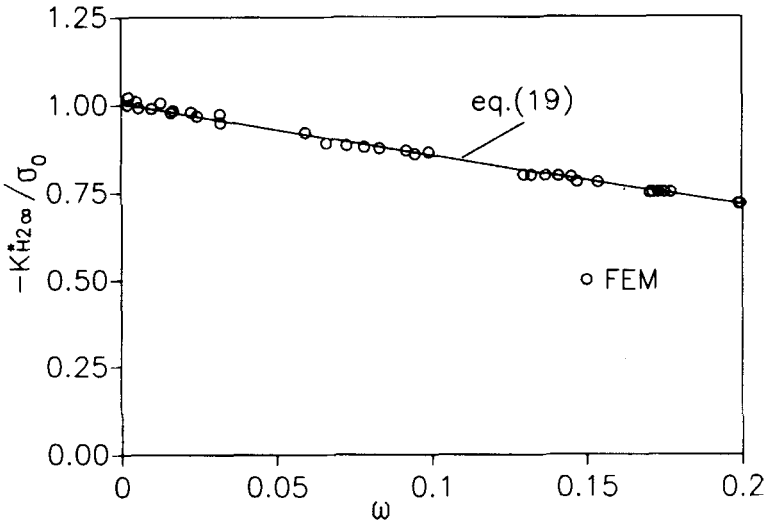

FIGURE 7a Values of $-K^*_{H2\infty}/\sigma_0$ *versus* ω for bimaterials with the Poisson's ratio $\nu_2 = 0.2$.

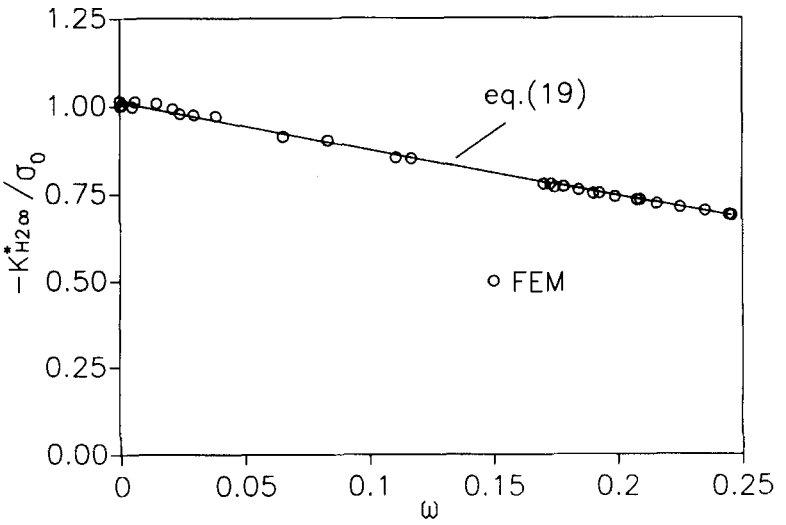

FIGURE 7b Values of $-K^*_{H2\infty}/\sigma_0$ *versus* ω for bimaterials with the Poisson's ratio $\nu_2 = 0.25$.

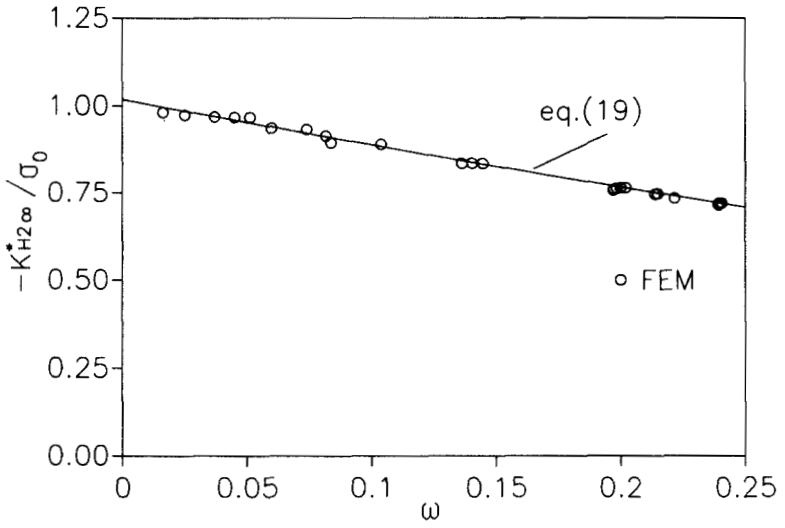

FIGURE 7c Values of $-K^*_{H2\infty}/\sigma_0$ *versus* ω for bimaterials with the Poisson's ratio $v_2 = 0.3$.

Poisson's ratios of $v_2 = 0.2$, 0.25 and 0.3. The values of $-K^*_{H1\infty}/\sigma_0$ are fitted with a polynomial in ω and v_2:

$$-K^*_{H1\infty}/\sigma_0 = 0.9919 + 0.1523\,v_2 - 2.3825\,\omega - 8.0247\,v_2\omega - 0.5966\,v_2^2 + 14.5589\,v_2^2\omega + 15.3373\,\omega^2 - 16.7054\,v_2\omega^2 - 3.5281\,v_2^2\omega^2 \quad (20)$$

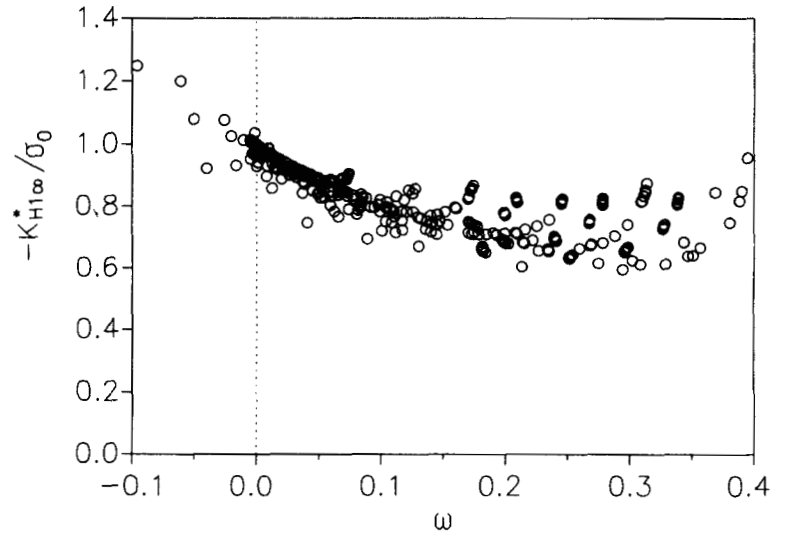

FIGURE 8 The values of $-K^*_{H1\infty}/\sigma_0$ *versus* ω.

The values of eq. (20) are also shown as solid lines in Figure 9a–9c. The maximum relative error $(K^{*FE}_{H1\infty} - K^{*}_{H1\infty})/K^{*}_{H1\infty}$ between the results obtained using the FE method and Eq. (20) is smaller than 10%.

It can be seen that the ratios $-K^{*}_{H1\infty}/\sigma_0$ and $-K^{*}_{H2\infty}/\sigma_0$ depend on v_2 and only negligibly on v_1. This means that the Poisson's ratio of the material with the smaller

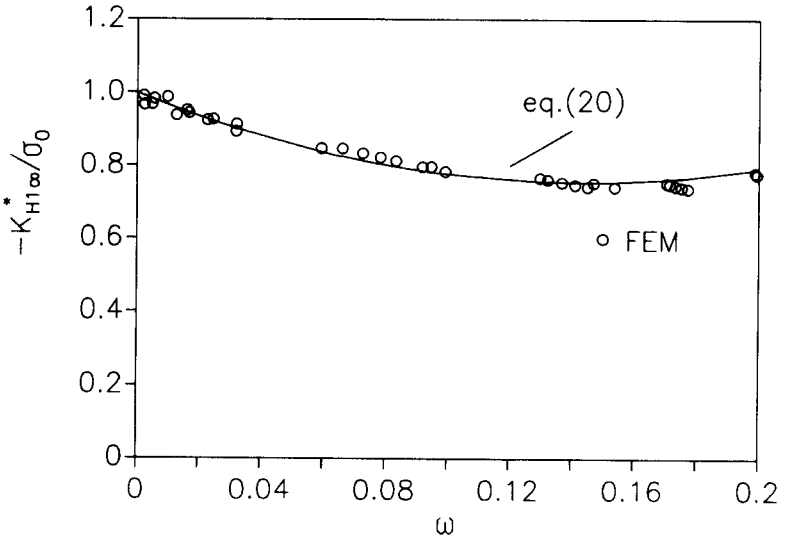

FIGURE 9a Values of $-K^{*}_{H1\infty}/\sigma_0$ *versus* ω for bimaterials with the Poisson's ratio $v_2 = 0.2$.

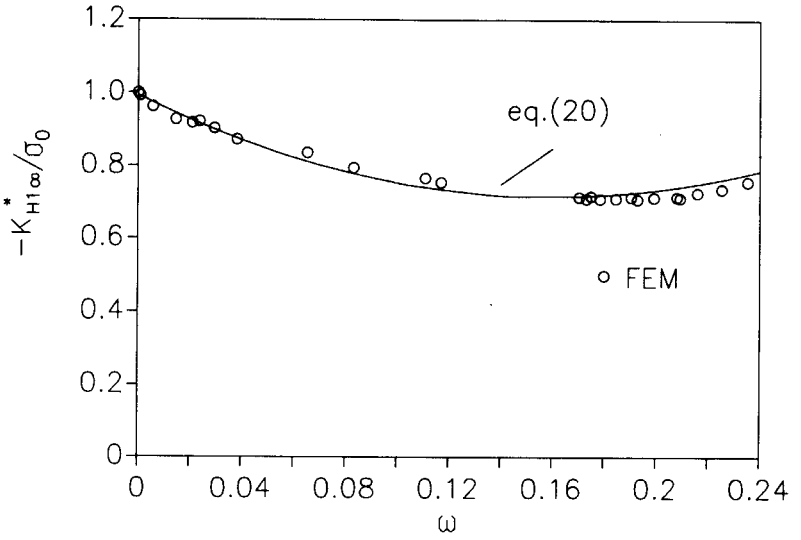

FIGURE 9b Values of $-K^{*}_{H1\infty}/\sigma_0$ *versus* ω for bimaterials with the Poisson's ratio $v_2 = 0.25$.

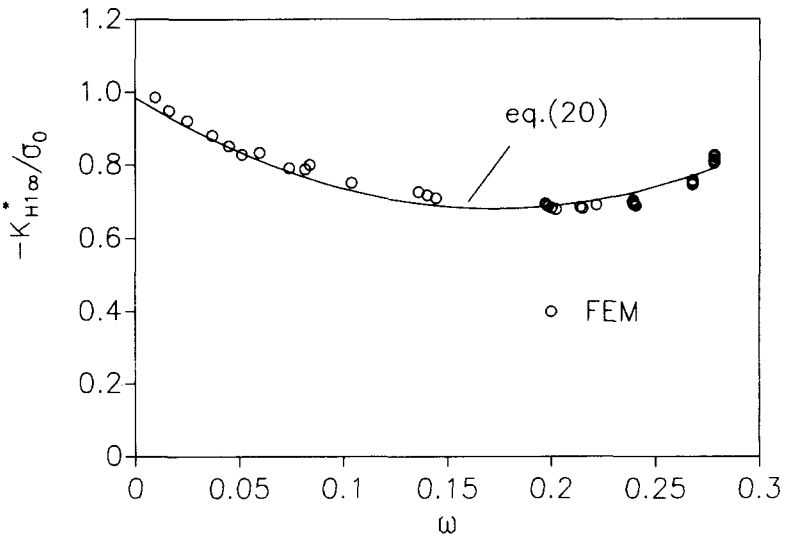

FIGURE 9c Values of $-K^*_{H1\infty}/\sigma_0$ *versus* ω for bimaterials with the Poisson's ratio $\nu_2 = 0.3$.

effective Young's modulus ($E_2^* < E_1^*$) is more important than the Poisson's ratio of the material with the larger effective modulus.

THE EXPONENT n

We define the value of $K_{H1\infty} = K_{H2\infty}$ for $H_1/H_2 = 1$ as $\bar{K}_{H\infty}$. The stress intensity factor $\bar{K}_{H\infty}$ is calculated with the method described before. The ratios are $H_1/H_2 = 1$ and $L/H_2 = 100$. The material parameters of the joints investigated are:

$$E_1 = 1 \times 10^5 \text{MPa} \qquad 0.2 \le \nu_1 \le 0.4 \quad \alpha_1 = 1 \times 10^{-6}\,\text{K}^{-1}$$

$$1 \times 10^3 \text{MPa} \le E_2 \le \frac{\nu_2(1+\nu_2)}{\nu_1(1+\nu_1)} E_1 \qquad 0.2 \le \nu_2 \le 0.4 \quad \alpha_2 = 2 \times 10^{-6}\,\text{K}^{-1}$$

The upper limit for E_2 is due to the restriction $\beta < \alpha/2$. Figure 10 shows the values of $-\bar{K}_{H\infty}/\sigma_0$ *versus* ω. The values of $-\bar{K}_{H\infty}/\sigma_0$ are fitted by a polynomial in ω,

$$\bar{K}_{H\infty} = 0.9981 - 2.7248\omega + 7.2521\omega^2 - 7.0352\omega^3. \tag{21}$$

Furthermore, Figure 10 shows the values of Eq. (6) for $-K_{L\infty}/\sigma_0$. It is shown that the statement in reference 6 $\bar{K}_{H\infty} = \bar{K}_{H2\infty}(H_1/H_2 = 1) = K_{L\infty}$ is only valid for small ω. For material combinations with a large stress exponents, ω, the divergence between $K_{L\infty}$ and $\bar{K}_{H\infty}$ reaches up to 25%.

For joints with $H_1/H_2 = 1$ and $H_1/L \le 0.1$ Eq. (15) can be written as follows:

$$\bar{K}_{H\infty} = K^*_{H2\infty}\left[1 - \exp\left\{-\left(\frac{K^*_{H1\infty}}{K^*_{H2\infty}}\right)^n\right\}\right]^{\frac{1}{n}} \tag{22}$$

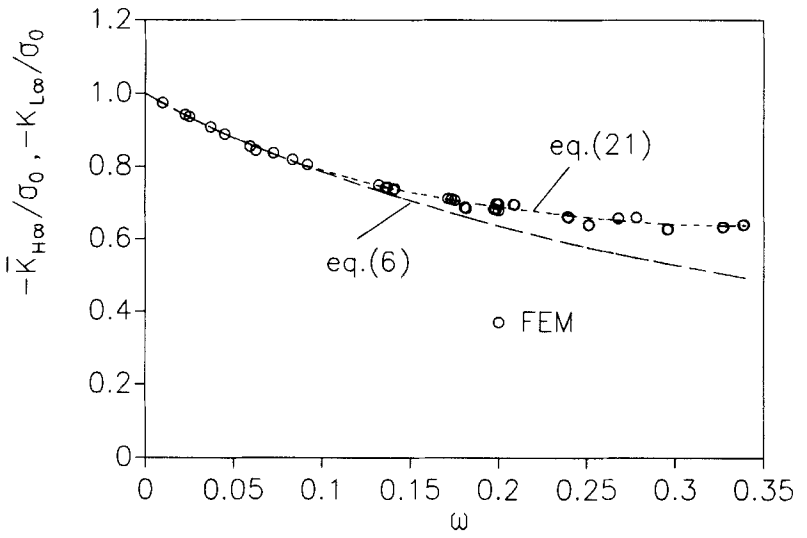

FIGURE 10 Values of $-\bar{K}_{H\infty}/\sigma_0$ and $-K_{L\infty}/\sigma_0$ *versus* ω.

If the polynomial descriptions of Eq. (19), Eq. (20) and Eq. (21) are used, a relationship results between n and ω with v_2 as the parameter. The solutions of n from Eq. (22) are shown in Figure 11 as points. The relationship between n, ω and v_2 is fitted by a polynomial using the least squares method:

$$n = 48.2878 - 110.723\,v_2 - 479.042\,\omega - 340.791\,v_2\omega + 1200.72\,v_2^2 - 3377.91\,v_2^2\omega + 2056.29\,\omega^2 - 3025.53\,v_2\omega^2 + 5534.08\,v_2^2\omega^2 \tag{23}$$

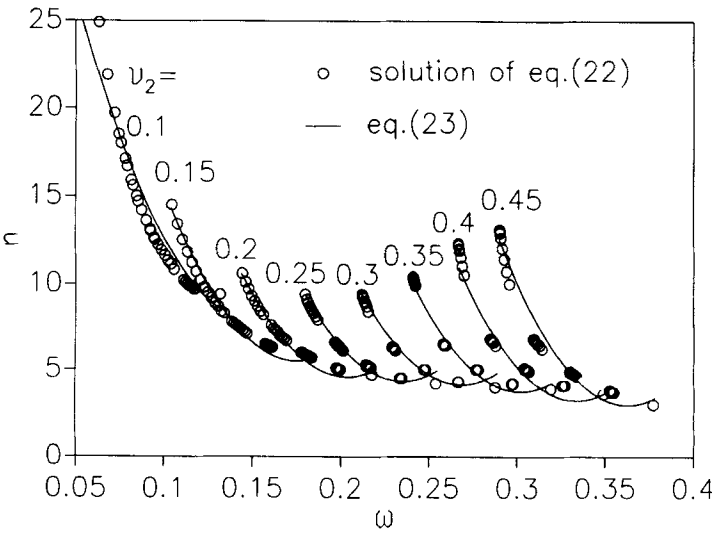

FIGURE 11 The relationship between n and ω with v_2 as the parameter.

Now, the four parameters $K_{L\infty}$, $K^*_{H2\infty}$, $K^*_{H1\infty}$ and n in Eq. (15) can be approximated by the equations (6), (19), (20), and (23). Therefore the stress field near the singular point can be calculated without any further FEM calculations.

EXAMPLES

Figure 12 shows the stress intensity factor, K_{H2}, for combination B with different geometries obtained by the finite element method as points and from Eq. (15) as solid lines. The values of Eq. (15) are in good agreement with the stress intensity factors obtained from the finite element method.

The stresses in the vicinity of the singular point are calculated by the finite element method and compared with those calculated with Eq. (1) using the stress intensity factor of equation (15). As examples, two combinations with a great and a small stress exponent ω are considered. The geometries and material parameters of the joints are shown in Table IIIa. The Dundurs parameters, the stress exponent, the regular stress term, and the angular functions for the investigated joints are shown in Table IIIb. The stress intensity factor and the parameters of geometry are shown in Table IIIc.

Figure 13a and 13b show the stresses, σ_{ij}, along the interface for the combinations C and D. The results of the finite element method are plotted as points, the values of Eq. (1) as solid lines.

Depending on the elastic constants and on the geometry, the relative error of the stress intensity factor goes up to 10%. The accuracy achieved in determining the stresses near the singular point depends not only on the relative error of the stress

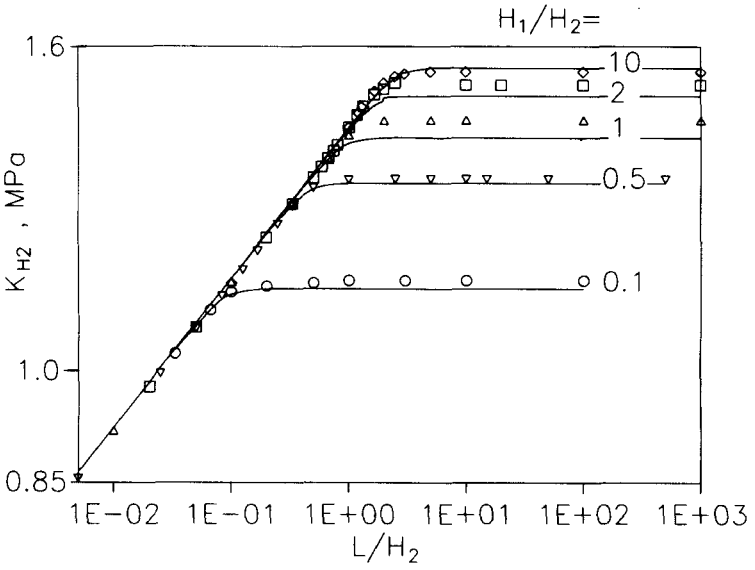

FIGURE 12 The values of $\log(K_{H2})$ obtained by the finite element method and by Eq. (15) *versus* $\log(L/H_2)$ for combination B.

TABLE IIIa
Geometry and material parameters of combinations C and D

Combination	$\frac{H_1}{H_2}$	$\frac{L}{H_2}$	E_1 in GPa	E_2 in GPa	ν_1	ν_2	α_1 in $10^{-6}K^{-1}$	α_2 in $10^{-6}K^{-1}$
C	100	100	270	140	0.37	0.28	1	2
D	0.01	1	180	60	0.2	0.35	1	2

TABLE IIIb
The Dundurs parameters, the stress exponent, the regular stress term, and the angular functions of combinations C and D

Combination	α	β	ω	σ_0 in MPa	$f_{y0°}$	$f_{y45°}$	$f_{y90°}$
C	0.3463	0.1382	0.01991	−1.7434	1.0	1.0224	1.1088
D	0.4656	0.06889	0.1027	−0.2293	1.0	1.1004	1.5354

TABLE IIIc
The stress intensity factors of combinations C and D

Combination	K_{H2}^{FE} in MPa	K_{H2}^{analyt} in MPa	$K_{L\infty}$ in MPa	$K_{H1\infty}^{*}$ in MPa	$K_{H2\infty}^{*}$ in MPa
C	1.7097	1.7219	1.6502	1.6081	1.7225
D	0.1064	0.1025	0.1790	0.1646	0.2054

intensity factor, but also on the stress exponent, ω, the ratio, $-K_{H2}/\sigma_{ij0}$, the angular function, f_{ij}, and the relative distance, (r/H_2).

If $\Delta\sigma_{ij}$ is the absolute error of the stress σ_{ij} and ΔK_{H2} is the absolute error of the stress intensity factor K_{H2}, there results

$$\frac{\Delta\sigma_{ij}}{\sigma_{ij}} = \frac{\Delta K_{H2}}{K_{H2}} \frac{1}{1 + \dfrac{\sigma_{ij0}(\theta)}{K_{H2}} \dfrac{1}{f_{ij}(\theta)} \left(\dfrac{r}{H_2}\right)^{\omega}}. \tag{24}$$

The regular stress terms σ_{x0} and σ_{xy0} vanish. Therefore,

$$\frac{\Delta\sigma_x}{\sigma_x} = \frac{\Delta\sigma_{xy}}{\sigma_{xy}} = \frac{\Delta K_{H2}}{K_{H2}}. \tag{25}$$

Only the relative error of the stress σ_y depends on the coordinates r and θ and on the stress exponent ω.

For $\omega \to 0$ there is $f_{ij}(\theta) \to 1$ and $\sigma_{y0}/K_{H2} \to -1$ and, therefore, $\Delta\sigma_y/\sigma_y \to \infty$. Because of that, it is not recommended to use the developed relations for the stress σ_y for small exponents ω. From our calculations we recommend a lower limit of $\omega = 0.01$. If the Poisson's ratios are within 0.2 and 0.35, then the ratio of the Young's moduli should be $E_1/E_2 > 2.3$ or $E_1/E_2 < 0.4$.

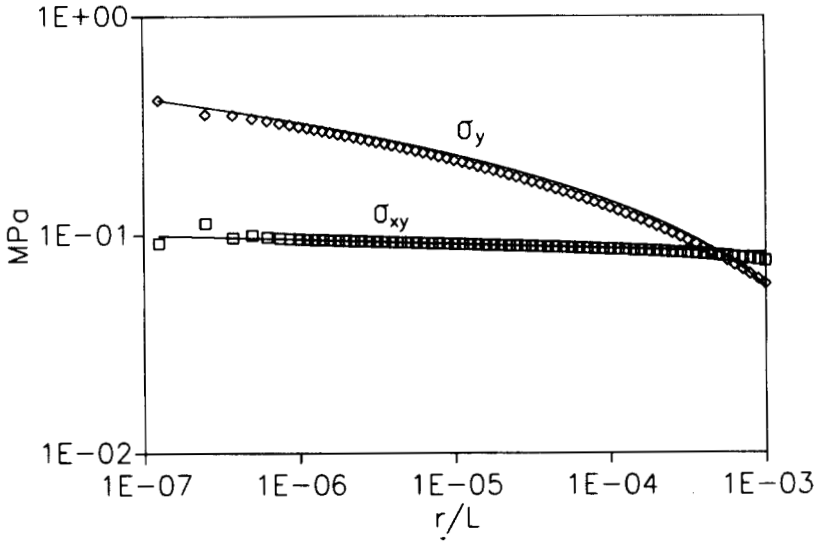

FIGURE 13a The stresses $\log(\sigma_y)$ and $\log(\sigma_{xy})$ *versus* $\log(r/L)$ along the interface of combination C.

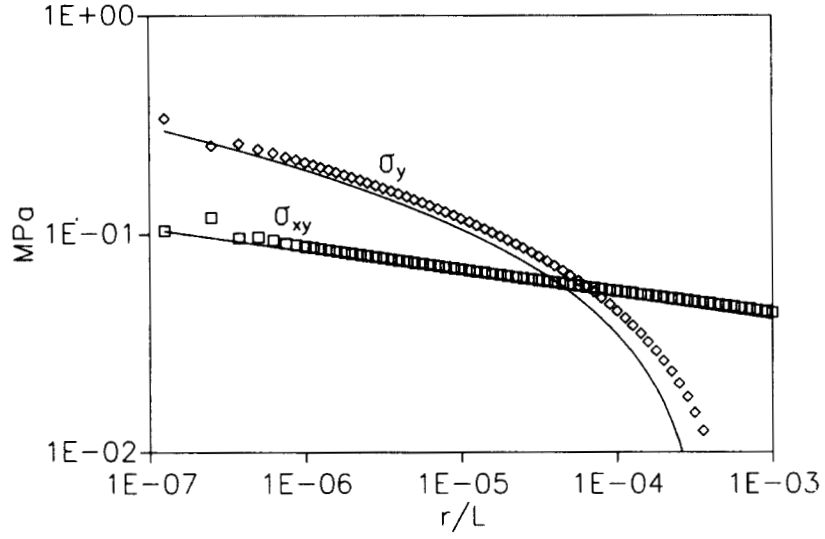

FIGURE 13b The stresses $\log(\sigma_y)$ and $\log(\sigma_{xy})$ *versus* $\log(r/L)$ along the interface of combination D.

CONCLUSION

In two bonded dissimilar materials high stresses can occur in the intersection between the interface and the free edge after a uniform change in temperature. The stress field in this area can be described by the sum of a singular stress term and a regular stress term. With the exception of the stress intensity factor all parameters in Eq. (1) can be calculated analytically.

The stress intensity factor of the singular term depends on the geometry, the elastic constants, the thermal expansion coefficients and the loading of the bimaterial. The stress intensity factor can be calculated by using the finite element method. For joints with an extreme geometry the upper limits $K^*_{H1\infty}$ and $K^*_{H2\infty}$ were found for the stress intensity factors K_{H1} and K_{H2}. The relationship between the geometry of two bonded quarter planes and the stress intensity factor was evaluated and described by an exponential function using the constants $K^*_{H1\infty}$ and $K^*_{H2\infty}$ as parameters. $K^*_{H1\infty}$ and $K^*_{H2\infty}$ are characteristic quantities of each material combination and independent of geometry. The relationships between the elastic constants and $K^*_{H1\infty}$ and $K^*_{H2\infty}$ are described by polynomial functions.

The stress intensity factor can be calculated now with a maximum relative error of ten percent. For material combinations with relevance to practice the relative error is significantly smaller.

For joints with stress exponents ω greater than 0.01 the analytically-approximated stresses are in good agreement with the stresses calculated with the finite element method.

Acknowledgement

The financial support of the Deutsche Forschungsgemeinschaft is gratefully acknowledged.

References

1. S. Timoshenko, *J. Optical Socy. America*, **11**, 233 (1925).
2. M. S. Hess, *Int. J. of Fracture*, **3**, 262 (1969).
3. E. Suhir, *J. Appl. Mechanics*, **56**, 595 (1989).
4. M. L. Williams, *J. Appl. Mechanics*, **74**, 526 (1952).
5. D. B. Bogy, *J. Appl. Mechanics*, **38**, 377 (1971).
6. M. Heinzelmann, D. Munz, Y. Y. Yang, *Computational Materials Science*, **1**, 259 (1993).
7. D. Munz, Y. Y. Yang, *J. Appl. Mechanics*, **59**, 857 (1992).
8. K. Mizuno, K. Miyazawa, T. Suga, *J. of the Faculty of Eng., The Univ. of Tokyo* (B), **39**(4), 401 (1988).
9. J. Dundurs, *J. Appl. Mechanics*, **36**, 650 (1969).
10. Y. Y. Yang, Fortschritt-Bericht VDI, Reihe 18, No. 113, 1992.
11. M. Tilscher, D. Munz, Y. Y. Yang, *Int. J. of Fracture*, **65**, R23-R28, (1994).
12. ABAQUS USER'S MANUAL, Hibbitt, Karlsson and Sorensen, Inc. (1989).